Zhang et al. EURASIP J. Adv. Signal Process. (2021) 2021:72
https://doi.org/10.1186/s13634-021-00783-x

EURASIP Journal on Advances in Signal Processing

RESEARCH

Open Access

2-D DOA estimation method based on coprime array MIMO radar

Fei Zhang[1*], Zijing Zhang[1], Aisuo Jin[1], Chuantang Ji[1] and Yi Wang[2]

*Correspondence: zjzf@just.edu.cn
[1] School of Electronic and Information, Jiangsu University of Science and Technology, Zhenjiang 212003, China
Full list of author information is available at the end of the article

Abstract

Aiming at the problem that traditional direction of arrival (DOA) estimation methods cannot handle multiple sources with high accuracy while increasing the degrees of freedom (DOF), a new method for 2-D DOA estimation based on coprime array MIMO radar (SA-MIMO-CA) is proposed. First of all, in order to ensure the accuracy of multi-source estimation when the number of elements is finite, a new coprime array model based on MIMO (MIMO-CA) is proposed. This method is based on a new MIMO array-based co-prime array model (MIMO-CA), which improves the accuracy of multi-source estimation when the number of array elements is limited, and obtains a larger array aperture with a smaller number of array elements, and improves the estimation accuracy of 2-D DOA. Finally, the effectiveness and reliability of the proposed SM-MIMO-CA method in improving the DOF of array and DOA accuracy are verified by experiments.

Keywords: Two-dimensional DOA, MIMO, Coprime array, Sparse array, Compressed sensing

1 Introduction

The traditional direction of arrival (DOA) method generally uses a uniform linear array, and the number of estimable target sources is less than the number of array elements. Classical methods such as multiple signal classification (MUSIC) method [1–3] or estimation of signal parameters via rotational invariance techniques (ESPRIT) method [4, 5] use N array elements to estimate at most N-1 target signals, and the degree of freedom of the array is limited. Therefore, in the case of a certain number of array elements, how to optimize the array structure to obtain a larger array aperture to improve the DOA estimation accuracy and multi-target resolution has always been a hot issue for scholars [6–8].

In recent years, with the continuous in-depth study of the array element structure, domestic and foreign scholars have proposed many non-uniform array structures [9–11]. For example, the nested array structure can estimate up to 2N signal sources by using N array elements. The nested array is not only easy to construct, but also easy to obtain the specific position of the array element and higher array freedom. However, because the distance between some elements in the nested array is very small, mutual coupling between the antennas will be caused, thereby affecting the performance of the array DOA estimation. With the appearance of the co-prime array structure, the effect of mutual coupling between antennas in nested arrays has been solved by it. At the same time, the degree of freedom of the array is greatly improved by increasing the difference information of the array element position [12–15]. Although the traditional DOA method can easily be extended to two dimensions to deal with a planar array or a circular array, the traditional DOA method uses a parallel uniform linear array composed of several linear sub-arrays, which leads to a problem of large computational complexity. In order to improve the accuracy of two-dimensional DOA estimation, anti-interference, etc., a multi-input multiple-output (MIMO) radar is proposed. MIMO radar uses multiple antennas to transmit different waveforms and receive reflected signals from multiple targets. Therefore, it can achieve large degrees of freedom (DOF) based on waveform diversity, thereby improving spatial resolution, enhancing parameter identification, and improving target detection performance [16–20]. The method that Li et al. proposed [21, 22] combines MIMO and coprime array to estimate DOA, which improves the estimation performance of DOA. However, the uniform linear arrays were still used as coprime array to construct effective differential arrays with ideal characteristics, which can only provide one-dimensional DOA estimation; as a result, the accuracy of two-dimensional DOA estimation is not very high. Therefore, this paper proposes a new coprime array model based on MIMO (MIMO-CA). To improve the accuracy of two-dimensional DOA estimation, the transmitting array of the array combination is a special irregular array, and the receiving array is a uniform linear array.

Bautista and Buck et al. [23] proposed the use of compressed sensing for sparse matrix processing, which reduces the computational complexity of DOA estimation, but it is not used in the MIMO coprime array structure. So et al. [24] proposed a fast DOA estimation method with parallel uniform linear arrays, which constructs a sub-array, but when there are many sources, additional matching is required, and the sensors are not fully utilized. Tayem et al. [25, 26] proposed a new array, that is, each of the three parallel sub-arrays is consistent, but it is impossible to detect more sources under the same number of array elements. Therefore, on the basis of the new array combination method (MIMO-CA) proposed in this paper, it combines the methods of compressed sensing [27–30] and proposes a new two-dimensional DOA method, that is, a new method for 2-D DOA estimation based on coprime array MIMO radar (SA-MIMO-CA). First of all, this method can be realized by constructing an equivalent array of sparse array, that is, using the sparse array topology of virtual array elements to analyze a larger number of two-dimensional DOA sources, and can automatically match the corresponding azimuth and elevation angles. Besides, by transforming the two-dimensional DOA estimation into two independent one-dimensional DOA estimation problems, only one variable can be estimated, thus reducing the computational complexity. Then, when the number of information sources is greater than or equal to the number of array elements, a virtual differential array is established, and sparse reconstruction and least squares operations are performed. The sparse matrix is processed through the compressed sensing method, so that $M+4$ array elements can identify $2M^2$ sources. Finally, experiments verify the validity and reliability of SA-MIMO-CA for 2-D DOA estimation.

The content of this paper is mainly structured as follows. Section 2 gives the array configuration and signal model of the SA-MIMO-CA method. Section 3 gives the DOA

Table 1 Main contributions

The serial number	Content
1	A new mutual-prime array model is proposed
2	A new 2 D DOA estimation method is proposed

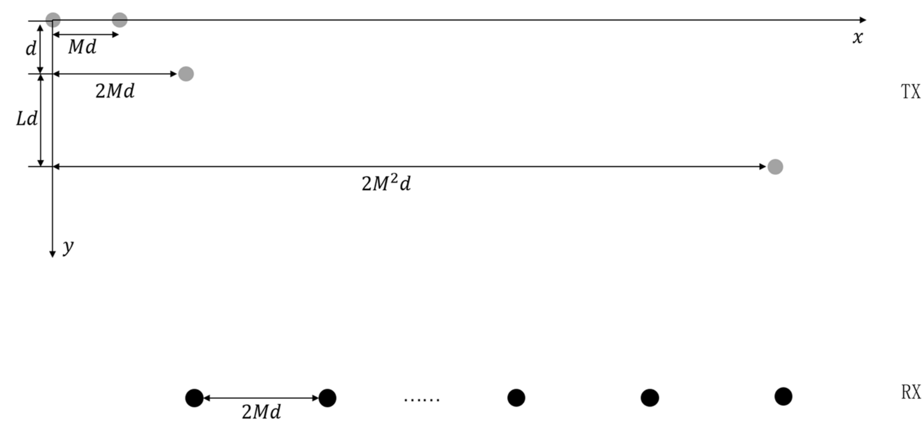

Fig. 1 MIMO coprime array model

estimation method based on the sparse array. Section 4 gives the experimental results and analysis (Table 1).

2 Preliminaries

In this section, the array model and signal model of this article are mainly given.

2.1 Array model

As shown in Fig. 1, MIMO targets 4 transmit arrays and M receive arrays, that is, the total number of arrays is $M+4$. Due to the nature of the MIMO array model, the array can be virtualized so that the number of virtualized arrays is $4M$. The array arrangement of the transmitting array is shown in Fig. 1, and the receiving array is M uniform linear arrays with a spacing of $2Md$ along the x-axis direction, where $d = \lambda/2$ and λ is wavelength.

Due to the nature of the MIMO radar, the virtual array is shown in Fig. 2.

Due to the need to construct a coprime array, the last element of sub-array 2 is discarded to form a coprime array, as shown in Fig. 3.

As shown in Fig. 3, the coprime array consists of three sparse linear uniform arrays. Sub-array 1 has *2 M* array elements, and its array element spacing is *Md*; and sub-arrays 2 and 3 have *M-1* and M array elements, and its array element spacing is. The array element spacing d is $\lambda/2$, where λ is the wavelength of the corresponding carrier frequency. By choosing $M \in \mathbb{N}^+$ and $2M \in \mathbb{N}^+$ to be relatively prime (where $\mathbb{N}^+$ is expressed as a

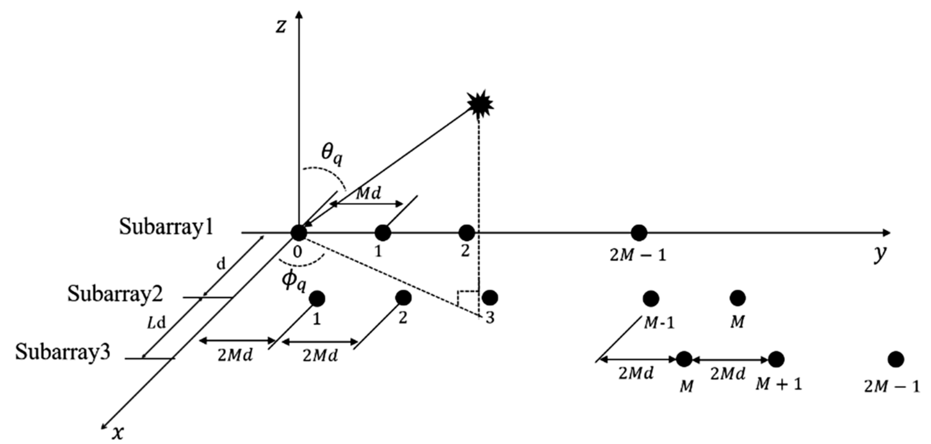

Fig. 2 MIMO array model after virtual

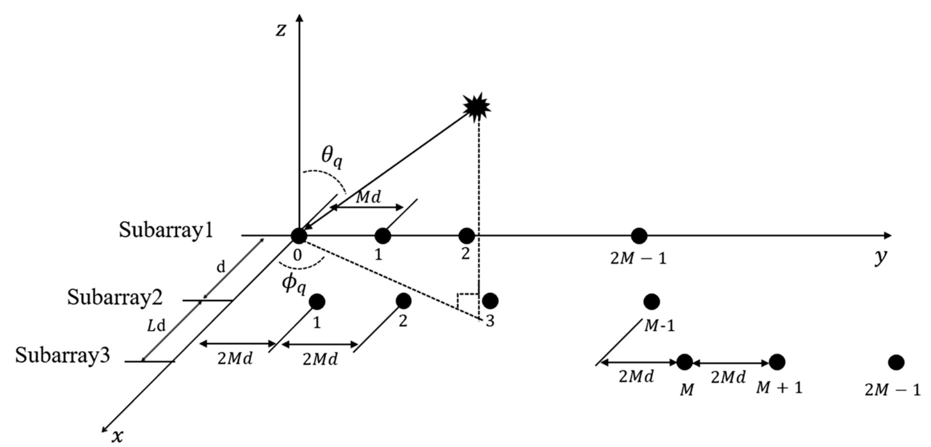

Fig. 3 Virtual post-coprime MIMO array

set of positive integers), the minimum cell spacing along the y-axis is $\lambda/2$. This article assumes that the array sensor is located at

$$\left\{ (x, y) | (0, M2md) \cup (d, 2Mm_1d) \cup \left(d + Ld, 2M^2d + 2Mm_2d \right) \right\} \tag{1}$$

where $2m \in [0, 2M-1]$, $m_1 \in [1, M-1]$, $m_2 \in [0, M-1]$, $n, m_1, m_2 \in \mathbb{N}^+$, where (x,y) represents the coordinates in the $x-y$ plane. To make the distinction simple, let $2M = N$. Then the array sensor is located at

$$\left\{ (x, y) | (0, M2md) \cup (d, Nm_1d) \cup (d + Ld, MNd + Nm_2d) \right\} \tag{2}$$

2.2 Signal model

For the estimation of the one-dimensional wave arrival angle direction, compared with the traditional coprime array, the main difference is that these sub-arrays are no longer collinear, and are placed in parallel at distances d and Ld, $\left(L \in \mathbb{N}^+\right)$, that is, the minimum unit spacing d along the x-axis. As L increases, the aperture of the array also increases, and the resolution also increases. But the larger the aperture, the signal will be correlated, so the value of L should not be very large.

The output is

$$\begin{aligned} x(l) = [&a_t(\theta_1,\varphi_1)\otimes a_r(\theta_1,\varphi_1), a_t(\theta_2,\varphi_2)\otimes a_r(\theta_2,\varphi_2),\ldots \\ &a_t(\theta_k,\varphi_k)\otimes a_r(\theta_k,\varphi_k)]S(l)+n(l) \end{aligned} \tag{3}$$

where θ_k and φ_k in Eq. (3) are the azimuth and elevation angles of the kth source, respectively. $\otimes$ is expressed as the Kronecker product. $n(l)$ is another noise vector whose elements are independently and evenly distributed in (i,i,d) and obey the Gaussian distribution $CN\left(0,\sigma_n^2 I_{N_t^i}\right)$, where $i=1,2,3$. $a_t(\theta_k,\varphi_k)=a_{ty}(\theta_k,\varphi_k)\otimes a_{tx}(\theta_k,\varphi_k)$, $a_r(\theta_k,\varphi_k)=a_{ry}(\theta_k,\varphi_k)\otimes a_{rx}(\theta_k,\varphi_k)$, where $a_{ty}(\theta_k,\varphi_k)$ and $a_{tx}(\theta_k,\varphi_k)$ are the steering vectors of the transmitting array. At the same time, $a_t(\theta_k,\varphi_k)\otimes a_r(\theta_k,\varphi_k)$ corresponds to the Kronecker product of the receiving direction vector and the sending direction vector of the kth target. $a_{ty}(\theta_k,\varphi_k)\otimes a_{tx}(\theta_k,\varphi_k)$ and $a_{ry}(\theta_k,\varphi_k)\otimes a_{rx}(\theta_k,\varphi_k)$ are the same. Let $a_{ti}(\theta_q,\varphi_q)\otimes a_{ri}(\theta_q,\varphi_q)=a_i(\theta_q,\phi_q)$, suppose the relationship after the virtual is:

$$x_i(t)=\sum\nolimits_{q=1}^{Q} a\left(\theta_q,\phi_q\right)e^{j2\pi\frac{x_i}{\lambda}\sin(\theta_q)\cos(\phi_q)}s_q(t)+n_i(t) \tag{4}$$

where

$$a_i\left(\theta_q,\phi_q\right)=\left[e^{j2\pi\frac{y_1^i}{\lambda}\sin(\theta_q)\cos(\phi_q)},\ldots,e^{j2\pi\frac{y^i_{t_t^i}}{\lambda}\sin(\theta_q)\cos(\phi_q)}\right]^T \tag{5}$$

Equation (5) represents (θ_q,ϕ_q) corresponding to the steering vector of the ith sub-array, where $q=1,\ldots,Q$, $i=1,2,3$. $y_j^i, 1\le j\le N_t^i$ is the y coordinate of the ith sensor. Where N_t^i is the total number of sensors in the ith sub-array, that is, $N_t^1=2M$, $N_t^2=M-1$, $N_t^3=M$.Similarly, x_i represents the position of the ith sub-array along the x-axis, and the noise vector element is in the ith sub-array $n_i(t)$, where (i,i,d) is independently and uniformly distributed and obeys the Gaussian distribution $CN\left(0,\sigma_n^2 I_{N_t^i}\right)$, where $i=1,2,3$. In order to transform the two-dimensional DOA estimation problem into two independent one-dimensional problems, as shown in Fig. 4, $\alpha_q,\beta_q\in[0°,180°]$, where q=1, …, Q, respectively, are expressed as the angle between the incident direction and the y-axis and x-axis The relationship between α_q,β_q and θ_q,ϕ_q is

$$\cos\left(\alpha_q\right)=\sin\left(\theta_q\right)\sin\left(\phi_q\right) \tag{6}$$

$$\cos\left(\beta_q\right)=\sin\left(\theta_q\right)\cos\left(\phi_q\right) \tag{7}$$

Therefore, the data vector received in Eq. (4) is

$$x_i(t)=\sum\nolimits_{q=1}^{Q} a_i\left(\alpha_q\right)e^{j2\pi\frac{x_i}{\lambda}\cos(\beta_q)}s_q(t)+n_i(t) \tag{8}$$

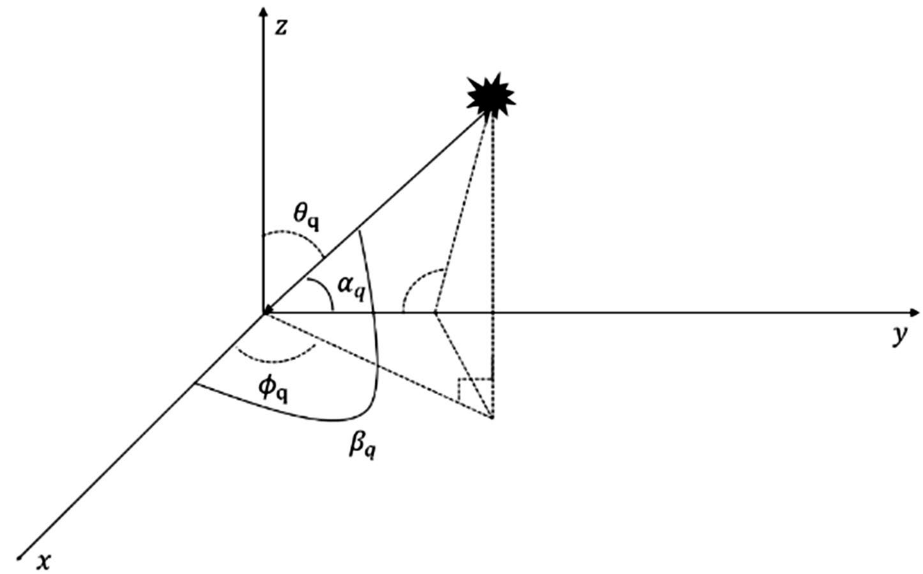

Fig. 4 (θ_q, ϕ_q) and (α_q, β_q) relationship diagram

The corresponding steering vector is

$$a_i(\alpha_q) = \left[e^{j2\pi \frac{y_i}{\lambda} \cos(\alpha_q)}, \ldots, e^{j2\pi \frac{y^i_{N_t}}{\lambda} \cos(\alpha_q)} \right]^T \tag{9}$$

Set $s(t) = [s_1(t), \ldots, s_Q(t)]^T$ to the signal vector, $A_i = [a_i(\alpha_1), \ldots, a_i(\alpha_Q)]$ is the array manifold corresponding to the ith sub-array, where $i = 1, 2, 3$, the data vector of the receiving channel can be written as

$$x_i(t) = A_i B_i s(t) + n_i(t) \tag{10}$$

The diagonal matrix is expressed as

$$B_i = \text{diag}\left(\left[e^{j2\pi \frac{x_i}{\lambda} \cos(\beta_1)}, \ldots, e^{j2\pi \frac{x_i}{\lambda} \cos(\beta_Q)} \right] \right) \tag{11}$$

Although traditional methods can achieve high-resolution DOA estimation, the $Q < N_t Q$ conditions must be met to obtain the noise subspace. In application, the problem of detecting information sources with more than the number of array elements has become the focus of research. In this section, an effective method is proposed to achieve the equivalence of differential arrays with a larger number of DOF. In addition, the group sparse array technology is used to improve the estimation accuracy of DOA, and the differential covariance equations of $x_i(t)$ and $x_k(t)$ are constructed.

The cross-covariance matrix of the data vectors accepted by subarrays $x_i(t)$ and $x_k(t), 1 \leq i, k \leq 3$ can be obtained. The cross-covariance matrix is

$$\begin{aligned} R_{x_{ik}} &= E\left[x_i(t)X_k^H(t)\right] \\ &= \sum_{q=1}^{Q} \sigma_q^2 e^{j2\pi \frac{(x_i-x_k)}{\lambda}} a_i(\alpha_q) a_k^H(\alpha_q) + n_i(t) n_k^H(t) \\ &= \begin{cases} A_i R_{ss} D_{ik} A_k^H & i \neq k \\ A_i R_{ss} A_i^H + \sigma_n^2 I_{N_t^i}, & i = k \end{cases} \end{aligned} \tag{12}$$

where $R_s = E[s(t)s^H(t)] = \text{diag}([\sigma_1^2, \ldots, \sigma_Q^2])$ is the covariance matrix of the $Q \times Q$ dimensional signal, and its diagonal term represents the scattered power of the signal. In addition,

$$D_{ik} = B_i B_k^H = \text{diag}\left\{ \left[e^{j2\pi \frac{(x_i-x_k)}{\lambda} \cos(\beta_1)}, \ldots, e^{j2\pi \frac{(x_i-x_k)}{\lambda} \cos(\beta_Q)} \right]^T \right\} \tag{13}$$

When $i = k$, it becomes the identity matrix.

The matrix $R_{x_{ik}}$ is quantized to obtain the following measurement vector:

$$z_{ik} = \text{vec}\left(R_{x_{ik}}\right) = \begin{cases} \overline{A}_{ik} b_{ik}, & i \neq k \\ \overline{A}_{ik} b_{ik} + \sigma_n^2 i, & i = k \end{cases} \tag{14}$$

where

$$\overline{A}_{ik} = \left[\overline{a}_{ik}(\alpha_1), \ldots, \overline{a}_{ik}(\alpha_Q)\right] \tag{15}$$

$$b_{ik} = \left[\sigma_1^2 e^{j2\pi \frac{(x_i-x_k)}{\lambda} \cos(\beta_1)}, \ldots, \sigma_1^2 e^{j2\pi \frac{(x_i-x_k)}{\lambda} \cos(\beta_Q)} \right]^T \tag{16}$$

where $\overline{a}_{ik}(\alpha_q) = a_i(\alpha_q) \otimes a_k^*(\alpha_q)$, $1 \leq q \leq Q$, $(\cdot)^*$ is denoted as conjugate. $i = \text{vec}(I_{N_t^i})$, using the van der Monte structure of vectors $a_i(\alpha_q)$ and $a_k(\alpha_q)$, the entry in $\overline{a}_{ik}(\alpha_q)$ retains the $e^{j\pi(Mn-Nm)} \cos(\alpha_q)$ factor. Therefore, z_{ik} can be regarded as a data vector received from a single snapshot signal vector b_{ik}, and the array manifold A_{ik} corresponds to a virtual array whose virtual elements are located in the self-hysteresis and cross-lag between different sub-array sets. Due to the relative prime properties of M and N, there are fewer redundant elements in these virtual arrays. Therefore, the degree of freedom in the common array is greatly increased, so that more sources of N_t can be estimated with fewer array elements.

3 Methods

On the basis of the array model and signal model proposed in Sect. 2, this section proposes a two-dimensional DOA estimation method based on a sparse array to ensure the performance of fine processing of multiple sources while increasing the degree of freedom.

3.1 2-D DOA estimation method for sparse array

Based on the MIMO-CA array model and signal model mentioned in Sect. 2, the signal vector in Eq. (14), $Z_{ik,} 1 \leq i, k \leq 3$, can be sparsely expressed on the entire discrete angle grid as

$$z_{ik} = \begin{cases} \overline{A}_{ik}^{\circ} b_{ik}^{\circ}, & i \neq k \\ \overline{A}_{ik}^{\circ} b_{\mathrm{ik}}^{\circ} + \sigma_n^2 i, & i = k \end{cases} \tag{17}$$

where $\overline{A}_{ik}^{\circ}$ is defined as the grid $\alpha_g, g = 1, \ldots, G_\alpha$ where $\overline{a}_{ik}(\alpha_g)$ is located, where $G_\alpha \gg Q$; b_{ik}° is a sparse vector, and its nonzero entry position corresponds to the DOA estimated by α_q, where $q = 1, \ldots, Q$. For different sub-arrays, nonzero items usually have different values, but share the same position when searching. In other words, b_{ik}° exhibits a set of sparsity on all pairs of sub-arrays. Therefore, the estimation of $\alpha_q, q = 1, \ldots, Q$, which can be solved in the sparse reconstruction framework [23], making full use of all the DOF of mutual lag and cross lag. Many effective methods in the framework of convex optimization [27, 28] and Bayesian sparse learning [29] can be used to solve the sparse reconstruction problem of complex-valued groups [29, 30]. In this paper, the complex multi-task Bayesian compressed sensing method is introduced into the SA-MIMO-CA method, mainly because the method has superior performance and robustness to solve the coherence problem, as follows,

In order to use self-lag and cross-lag, this paper replanned the vector z_{ik},

$$z_{ik} = \Phi_{ik}^{\circ} b_{ik}^{\circ} + \varepsilon_{ik}, \quad 1 \leq i, k \leq 3 \tag{18}$$

The respective steering matrix of each vector is

$$\Phi_{ik}^{\circ} = \begin{cases} \left[\overline{A}_{ik}^{\circ}, i\right], & i = k \\ \left[\overline{A}_{ik}^{\circ}, 0_{N_t^i N_t^k \times 1}\right], & i \neq k \end{cases} \tag{19}$$

The dimensionality of the unknown sparse vector is extended to $\overline{b}_{ik}^{\circ}$, and an additional element with a noise power of σ_n^2 is required. In this case, use $\overline{b}_{ik}^{\circ}$ to estimate that the first G_α is used to determine α_q, and discard the last element. In addition, the error vector ε_{ik} is included in (18) to illustrate the difference between the statistical expectation and the sample average when calculating the covariance matrix. The difference is modeled as i, i, d, and since a sufficient number of samples are used in the averaging, a Gaussian complex number is produced.

Suppose the elements in $\overline{b}_{ik}^{\circ}$ come from the product of the following zero-mean Gaussian distribution

$$\overline{b}_{ik}^{\circ g} \sim N\left(\overline{b}_{ik}^{\circ g} | 0, \gamma_g I_2\right), \quad g \in [1, \ldots, G_\alpha] \tag{20}$$

where $N(x|a, b)$ means that the random variable x follows the Gaussian distribution and the complex Gaussian distribution of the mean a and variance b, respectively. $\overline{b}_{ik}^{\circ g} = [\tilde{b}_{ik}^{\circ g_R} \tilde{b}_{ik}^{\circ g_I}]^T$ is a 2×1 vector composed of the real part coefficient $\tilde{b}_{ik}^{\circ g_R}$ and the imaginary part coefficient $\tilde{b}_{ik}^{\circ g_I}$, corresponding to the gth grid. It can be easily determined that when γ_g is set to 0, $\overline{b}_{ik}^{\circ g}$ approaches zero [30–33]. To achieve the sparsity of $\overline{b}_{ik}^{\circ}$, a Gamma prior is set to $\gamma_g^{-1} \sim \mathrm{Gamma}(\gamma_g^{-1} | a, b)$, where $\mathrm{Gamma}(x^{-1}|a, b) = \Gamma(a)^{-1} b^a x^{-(a-1)} \mathrm{e}^{-\frac{b}{x}}$ and $\Gamma(\cdot)$ are Gamma functions. a and b are hyperparameters. The vector $\gamma = [\gamma_1, \ldots, \gamma_G]^T$ contains $\overline{b}_{ik}^{\circ g}$, where $g = 1, \ldots, G_\alpha$ is shared with all groups to enhance sparsity. Similarly, the Gaussian prior is $N(0, \xi_0 I_2)$, ε_{ik} is set, and the Gamma prior is on ξ_0^{-1}, with hyperparameters c and d. Defining the density function of the two $G_a \times 1$ vectors $\overline{b}_{ik}^{\circ R} = [b_{ik}^{\circ 1k}, \ldots, b_{ik}^{\circ GR}]^T$ and $\overline{b}_{ik}^{\circ I} = [b_{ik}^{\circ 1I}, \ldots, b_{ik}^{\circ GI}]^T$ associated as $\overline{b}_{ik}^{\circ RI} = [(\overline{b}_{ik}^{\circ R})^T, (\overline{b}_{ik}^{\circ I})^T]^T$ can be evaluated as

$$P_r\left(\overline{b}_{ik}^{\circ RI} | \overline{z}_{ik}, \Phi_{ik}^{\circ}, \gamma, \xi_0\right) = \mathcal{N}\left(\overline{b}_{ik}^{\circ RI} | \mu_{ik}, \sum_{ik}\right) \tag{21}$$

where

$$\overline{z}_{ik}^{RI} = \left[\mathrm{Re}(z_{ik})^T, \mathrm{Im}(z_{ik})^T\right]^T \tag{22}$$

$$\mu_{ik} = \xi_0^{-1} \Sigma_{ik} \Psi_{ik}^T \overline{z}_{ik}^{RI} \tag{23}$$

$$\Sigma_{ik} = \left[\xi_0^{-1} \Psi_{ik}^T \Psi_{ik} + F^{-1}\right]^{-1} \tag{24}$$

$$\Psi = \begin{bmatrix} \mathrm{Re}\left(\Phi_{ik}^{\circ}\right) & -\mathrm{Im}\left(\Phi_{ik}^{\circ}\right) \\ \mathrm{Im}\left(\Phi_{ik}^{\circ}\right) & \mathrm{Re}\left(\Phi_{ik}^{\circ}\right) \end{bmatrix} \tag{25}$$

$$F = \mathrm{diag}\left(\gamma_1, \ldots, \gamma_G, \gamma_1, \ldots, \gamma_{G_\alpha}\right) \tag{26}$$

Obviously, when γ and ξ_0 are given, (23) and (24) can be used to derive the mean and variance of each scattering system in $\overline{b}_{ik}^{\circ RI}$. On the other hand, the values of γ and ξ_0 are determined by maximizing the logarithm of the edge likelihood, which can be achieved by the expectation maximization method to produce:

$$\gamma_g^{(new)} = \frac{1}{9} \sum\nolimits_{i,k=1}^{3} \left(\mathrm{Tr}\left[\Sigma_{ik} \Psi_{ik}^T \Psi_{ik}\right] + \left\|\tilde{z}_{ik}^{RI} - \Psi_{ik} \mu_{ik}\right\|_2^2\right) \tag{27}$$

$$\xi_0^{(new)} = \frac{1}{18 G_\alpha} \sum\nolimits_{i,k=1}^{3} \left(\mathrm{Tr}\left[\Sigma_{ik} \Psi_{ik}^T \Psi_{ik}\right] + \left\|\tilde{z}_{ik}^{RI} - \Psi_{ik} \mu_{ik}\right\|_2^2\right) \tag{28}$$

where $\mu_{ik,g}$ and $\mu_{ik,g+G_\alpha}$ are the gth and $g + G_\alpha$ th elements of the μ_{ik} vector, and $\Sigma_{ik,gg}$ and $\Sigma_{ik,(g+G_\alpha)(g+G_\alpha)}$ are the (g,g) and $(g + G_\alpha, g + G_\alpha)$ th elements in the matrix Σ_{ik}, because γ and ξ_0 depend on μ_{ik} and Σ_{ik}. Since CMT-BCS is iterative, iterate between (22)–(24) and (27)–(28) until the convergence criterion is reached. The estimated value $\hat{\alpha}_q, q = 1, \ldots, Q$ can obtain the maximum value of Q in $\sum_{i,k=1}^{3}\left(b_{ik}^{\circ gR} + b_{ik}^{\circ gI}\right), g = 1, \ldots, G$. Then the $Q \times 1$ vector in (14), that is, $b_{ik}, i \neq k$ can be estimated by least squares fitting, expressed as

$$\hat{b}_{ik} = \left(\hat{\overline{A}}_{ik}^H \hat{\overline{A}}_{ik}\right) \hat{\overline{A}}_{ik}^H z_{ik}, \quad i \neq k \tag{29}$$

where

$$\overline{A}_{ik} = \left[a_{ik}(\hat{\alpha}_1), \ldots, \overline{a}_{ik}(\hat{\alpha}_1)\right] \tag{30}$$

Therefore, $\beta_q, q = 1, \ldots, Q$ estimates to the following form

$$\hat{\beta}_q = \cos^{-1} - \left(\text{phase}\left(\hat{b}_q\right)/\pi\right) \tag{31}$$

where $\hat{b}_q$ is the qth element of vector $\hat{b}_{ik}$, so $\hat{\beta}_q$ automatically matches $\hat{\alpha}_q$. $\hat{\alpha}_q$ can be obtained in the same way. Therefore, according to Eqs. (6) and (7), $\hat{\theta}_q$ and $\hat{\phi}_q$ can be obtained.

$$\hat{\theta}_q = \sin^{-1}\left[\sqrt{\cos^2\left(\hat{\alpha}_q\right) + \cos^2\left(\hat{\beta}_q\right)}\right] \tag{32}$$

$$\hat{\phi}_q = \tan^{-1}\left[\frac{\cos\left(\hat{\alpha}_q\right)}{\cos\left(\hat{\beta}_q\right)}\right] \tag{33}$$

3.2 Steps of the SA-MIMO-CA method

The steps of the SA-MIMO-CA method are as follows:

Step1 Construct the MIMO array model to obtain the MIMO coprime array model in Fig. 1.
Step2 To obtain a coprime array, discard the last element of the second row of the virtual array, and get Eq. (3).
Step3 Use Eqs. (6) and (7) to turn the two-dimensional problem into two independent one-dimensional DOA estimation problems.
Step4 Use Eq. (12) to obtain the cross-covariance matrix $R_{x_{ik}}$ of the signal.
Step5 Use Eq. (14) to obtain the quantized measurement vector z_{ik}.
Step6 Use Eq. (18) to obtain the replanned z_{ik}.
Step7 Use Eqs. (29) and (30) to obtain $\hat{b}_{ik}$.
Step8 The two-dimensional DOA estimation of the N_t signals are obtained by matching Eqs. (32) and (33) (Fig. 5).

4 Results and discussion

This section mainly gives the experimental results and analysis. In this section, first of all, it is verified through experiments that the method in this paper is effective and reliable in improving the degree of freedom. Besides, it is verified through experiments that this article is effective and reliable in improving the performance of 2-D DOA estimation.

4.1 Degree of freedom analysis

In the case of one-dimensional, the obtained co-array is equivalent to the traditional coprime array, that is, the number of estimated signals can reach: $Q_{av} = MN$, that is, $Q_{av} = M^2$. For a given number of physical antennas $N_t = 2M + N - 1 = 4M - 1$, Q_{av} can be obtained in the following way

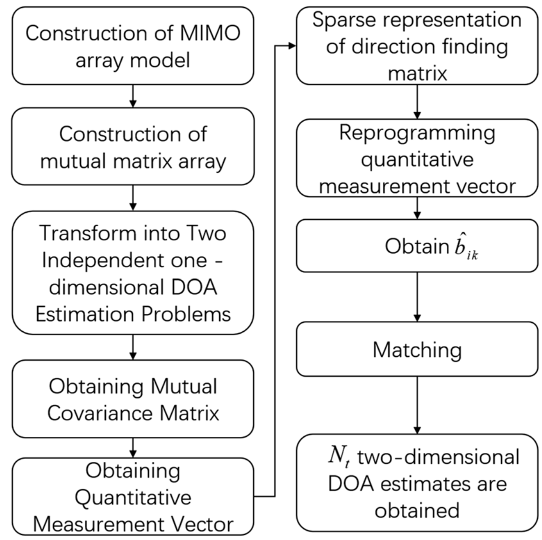

Fig. 5 Steps of the SA-MIMO-CA method

The maximum number of sources can be estimated: $Q_{av} = MN = M^2$

Restricted to $N_t = 2M + N - 1 = 4M - 1$

$M < N, M, N \in \mathbb{N}^+$

Obviously, the effective optimal coprime pair is that $2M$ and N are as equal as possible, that is, the array in this paper is selected as the optimal number of array elements. In this case, the maximum number of estimated signals Q_{av} is

$$Q_{\max} = \left[\frac{N_t(N_t + 2)}{8}\right] \tag{34}$$

As shown in Fig. 6, although the value of $Q_{\max}$ of all methods increases with the increase of N_t, it is obvious that the method based on the co-prime array (SA-MIMO-CA method, TDSR-CS method) is significantly better than other methods method. When $N_t > 6$, the method based on the relative prime array can resolve more sources than the number of other array sensors. For other methods, the number of resolvable sources is less than the number of sensors.

4.2 2-D DOA estimation performance comparison

4.2.1 The relationship between SNR and mean square error

Compare the SA-MIMO-CA proposed in this article with the TPAUL method, TDUL-PM method, TDSR-CS method and PUL-RARE method to verify two-dimensional DOA estimation performance of SA-MIMO-CA [26, 34–36]. Perform 100 Monte Carlo simulations for each method, and define the root mean square error as

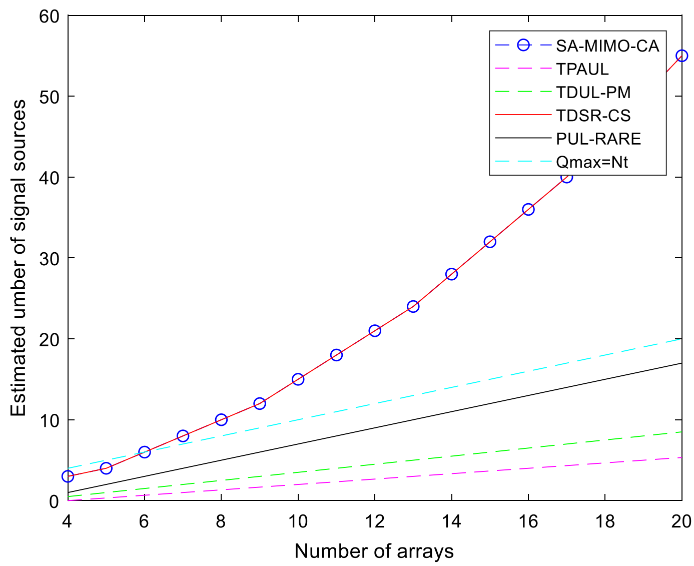

Fig. 6 The relationship between the number of arrays and the number of estimable sources

$$\mathrm{RMSE}_{\theta} = \sqrt{\frac{1}{IQ}\sum\nolimits_{i=1}^{I}\sum\nolimits_{q=1}^{Q}\left(\hat{\theta}_q(i) - \theta_q\right)^2} \tag{35}$$

$$\mathrm{RMSE}_{\phi} = \sqrt{\frac{1}{IQ}\sum\nolimits_{i=1}^{I}\sum\nolimits_{q=1}^{Q}\left(\hat{\phi}_q(i) - \phi_q\right)^2} \tag{36}$$

where I is the number of Monte Carlo experiments, and Q is the number of sources. We set $M=4$; that is, the array configuration of the $N_t = 4M - 1 = 15$ antenna. In addition, let $L=20$. Assume that Q far-field sources with the same power are on the elevation plane (θ_q, ϕ_q), where $\theta_q \in [0°, 90°]$, $\phi_q \in [-90°, 90°]$, $q = 1, \ldots, Q$. The grid interval in the angular space is set to 0.1°, and the parameter in the Bayesian sparse learning group is set to $a = b = c = d = 0$.

Figure 7 shows the SA-MIMO-CA method and TPAUL method, TDUL-PM method, TDSR-CS method, and PUL-RARE method when the number of sources $Q=3$ and the number of snapshots $T=500$ The estimated performance is compared, and the root mean square error (RMSE) changes of the method under different signal-to-noise ratio (SNR) are investigated. At the elevation angle, the performance of SA-MIMO-CA and PUL-RARE methods is close, but at the azimuth angle, when the SNR is 0, the performance of SA-MIMO-CA is improved by about 47.1% compared with the PUL-RARE method. Compared to the TPAUL method, it has increased by about 61.5%. By comparing RMSE under different SNR, it is concluded that SA-MIMO-CA has better estimation performance than several other methods under low SNR. Specific data are shown in Tables 2 and 3.

In different SNR comparisons, the lower the RMSE, the higher the resolution. It can be seen from Tables 2 and 3 and Fig. 7 that compared with other methods, the SA-MIMO-CA method has lower RMSE than other methods. Therefore, the resolution of the SA-MIMO-CA method is better in different SNR situations.

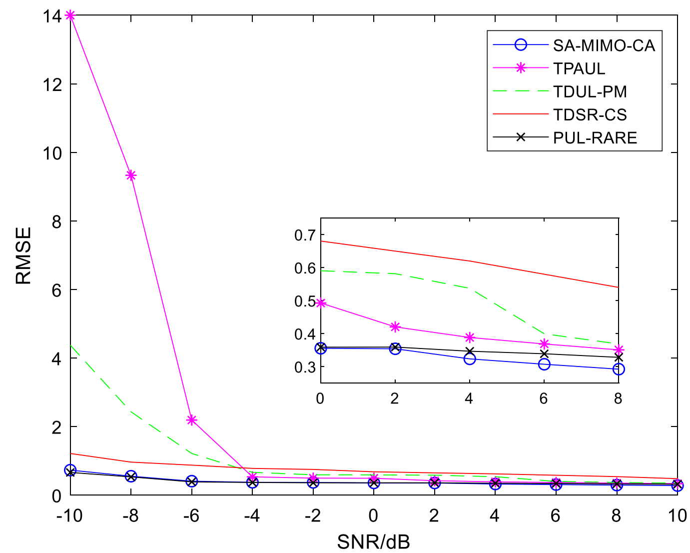

(a) The relationship between the SNR of the pitch angle and the RMSE of the pitch angle

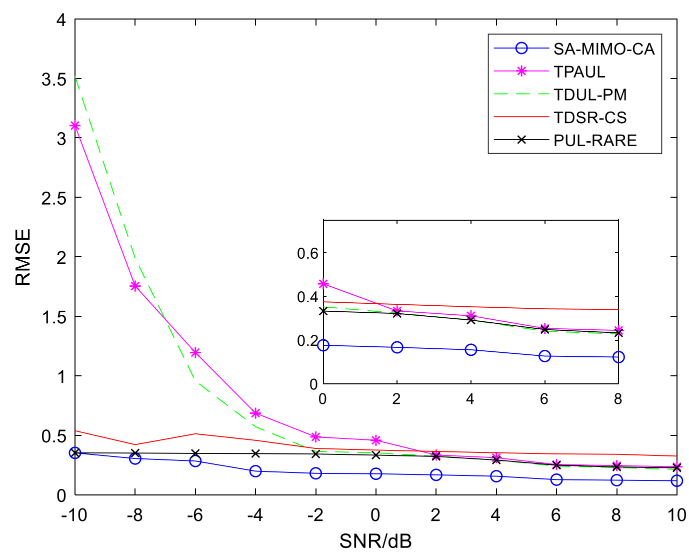

(b) The relationship between the SNR of the azimuth angle and RMSE of the azimuth angle

Fig. 7 The relationship between mean square error and SNR (the number of sources is 3)

Table 2 The relationship between the SNR of the elevation angle and the azimuth angle and the mean square error

	SA-MIMO-CA	TPAUL	TDSR-CS	TDUL-PM	PUL-RARE
Pitch angle (mean value of RMSE)	0.395	2.628	0.739	1.100	0.397
Azimuth (mean value of RMSE)	0.198	0.824	0.401	0.822	0.308

Table 3 The relationship between the SNR of the elevation angle and the azimuth angle and the mean square error (when the SNR is 0)

	SA-MIMO-CA	TPAUL	TDSR-CS	TDUL-PM	PUL-RARE
Mean square error of pitch angle	0.356	0.493	0.680	0.590	0.359
Azimuth mean square error	0.176	0.458	0.375	0.352	0.333

4.2.2 The relationship between angle and number of snapshots

Figure 8 shows that the SA-MIMO-CA method, TPAUL method, TDUL-PM method, TDSR-CS method and PUL-RARE method are used to estimate the position when the number of sources $Q=3$ and SNR $=0$. The performance comparison of each method, the comparison of RMSE under different snapshots. The overall performance of the SA-MIMO-CA method is improved by about 44.5% compared to the TPAUL method and about 23.4% compared with the PUL-RARE method. Experimental results show that SA-MIMO-CA performs better than TPAUL method and PUL-RARE method under different snapshots.

In different snapshots comparisons, the lower the RMSE, the higher the resolution. It can be seen from Table 4 and Fig. 8 that compared with other methods, the SA-MIMO-CA method has lower RMSE than other methods. Therefore, the resolution of the SA-MIMO-CA method is better in different SNR situations.

4.2.3 Comparison of 2-D DOA estimation

In the above two sets of experiments, the performance of the method at low signal sources was tested, and the comparison of different SNR and the mean square error of different snapshots proved the superiority of the method. Next, conduct a multi-source experiment. There are Q sources, the number of sources is greater than the number of arrays, the SNR is kept to 0, and the number of snapshots is set to 500, compared with the TDSR-CS method, as shown in Fig. 9.

Figure 9 shows the DOA estimation performance of each method, each of which represents the SA-MIMO-CA method in this paper, the actual value and the TDSR-CS method when the SNR$=0$, and the number of snapshots is 500. The DOA estimation result can be intuitively seen from Fig. 9 that SA-MIMO-CA is closer to the actual angle and has better two-dimensional DOA estimation performance.

4.2.4 Complexity analysis

Because SA-MIMO-CA method and TDSR-CS method can estimate more sources under the condition of finite array elements, while other methods can estimate less than SA-MIMO-CA method and TDSR-CS method under the same conditions as SA-MIMO-CA method and TDSR-CS method. The complexity of SA-MIMO-CA method and TDSR-CS method is compared. The complexity of TDSR-CS method is $O\left(NM^2+2M^3+\left(M^3+M^2\right)Q+M^3Q^3+L^3\right)$. The complexity of SA-MIMO-CA method is $O\left((4M-1)^2+2n^3+9Q^2\right)$. The time required for them is compared as

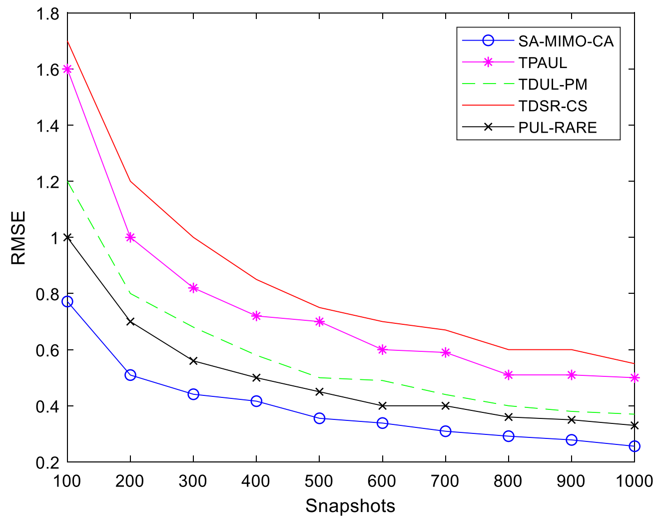

(a) The relationship between the mean square error of the pitch angle and the number of snapshots

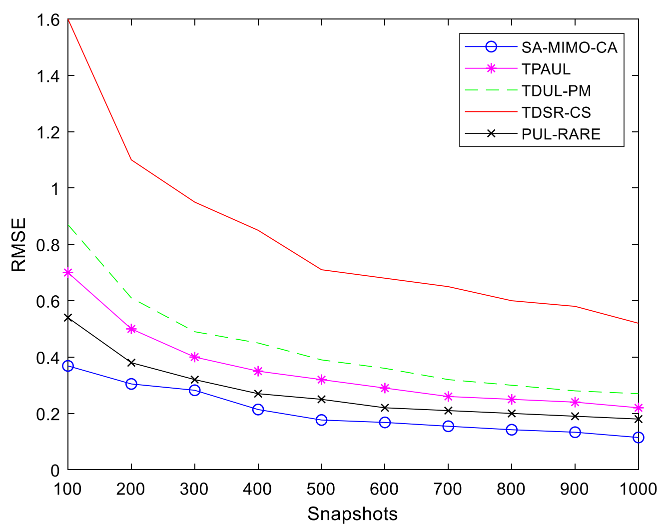

(b)The relationship between the mean square error of the azimuth angle and the number of snapshots

Fig. 8 The relationship between the mean square error and the number of snapshots (the number of sources is 3)

Table 4 Relationship between pitch angle, azimuth angle and the number of snapshots

	SA-MIMO-CA	TPAUL	TDSR-CS	TDUL-PM	PUL-RARE
Pitch angle (mean value of RMSE)	0.397	0.755	0.862	0.584	0.505
Azimuth (mean value of RMSE)	0.206	0.353	0.824	0.434	0.276

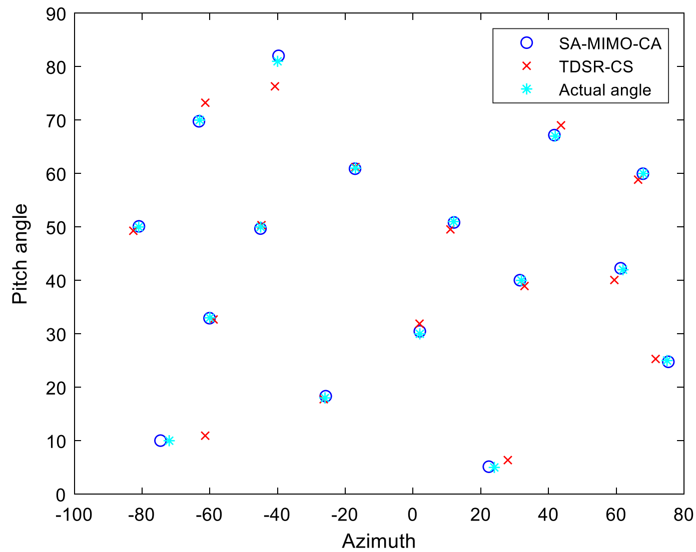

Fig. 9 Comparison of two-dimensional DOA estimation

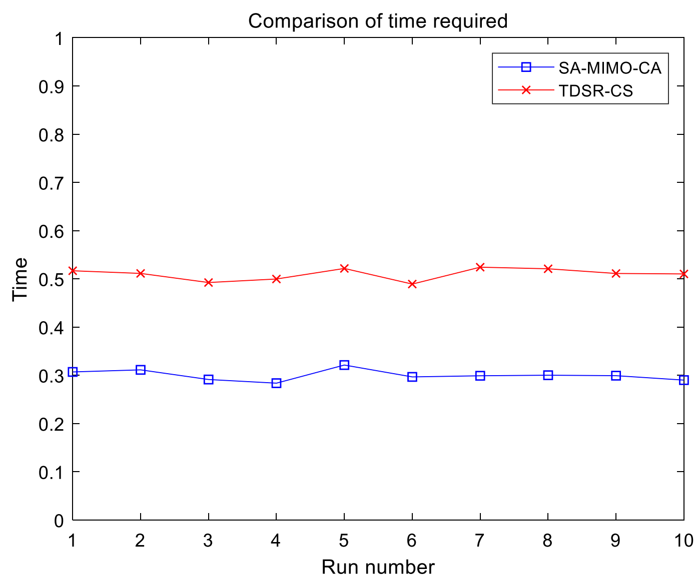

Fig. 10 Comparison diagram of the relationship between running times and time

shown in Fig. 10, from which it can be seen that SA-MIMO-CA method requires less time than TDSR-CS method.

5 Conclusion

Aiming at the problem that traditional array signal processing methods cannot handle multiple sources with high accuracy while increasing the degree of freedom, this paper proposes a new two-dimensional DOA estimation method based on MIMO radar coprime array. This method mainly uses the characteristics of coprime arrays and MIMO radars, which combines the theory of compressed sensing to improve the degree of freedom and accuracy of DOA estimation. Through experimental verification, compared with TPAUL method, TDUL-PM method, TDSR-CS method and PUL-RARE method, this method can effectively distinguish more signal sources. What's more, it has high two-dimensional DOA estimation accuracy and improves the degree of freedom of two-dimensional DOA estimation. Compared with TDSR-CS method, SA-MIMO-CA method reduces a certain amount of calculation. In the future, the processing of coherent sources and non-circular signals will be continue studied. The combination of Doppler frequency shift and angle measurement to further reduce the amount of calculation for target positioning will be considered. The applicability to colored noise will be considered.

Abbreviations

DOA: Direction of arrival; MUSIC: Multiple signal classification; ESPRIT: Estimation of signal parameters via rotational invariance technique; SNR: Signal-to-noise ratio; RMSE: The root mean square error; MIMO: Multiple-input multiple-output; MIMO-CA: Coprime array model based on MIMO; SA-MIMO-CA: The method of 2-D DOA estimation based on coprime array MIMO radar; TDUL-PM: Improved two-dimensional DOA estimation algorithm for two-parallel uniform linear arrays using propagator; TPAUL: An improved 2-D DOA estimation algorithm for three-parallel ULAs; PUL-RARE: A rank-reduction-based 2-D DOA estimation algorithm for three parallel uniform linear arrays; TDSR-CS: A SR-based 2-D DOA estimation algorithm using co-prime array.

Acknowledgements

The authors would like to thank Dayu Yin for his academic support, and I can finish the thesis successfully.

Authors' contributions

ZZJ analyzed and interpreted the data regarding the SA-MIMO-CA and was a major contributor in writing the manuscript. JAS and JCT analyzed the theory of compressed sensing and MIMO. ZF and WY provided experimental ideas. All authors read and approved the final manuscript.

Funding

This work was supported by the National Natural Science Foundation of China under Grant Nos. 61801170 and 61801435, Jiangsu Overseas Visiting Scholar Program for University Prominent Yong & Middle-aged Teachers and Presidents, the Scientific and Technological Key Project of Henan Province under Grant 212102210559 and in part by the Training Program for Young Scholar of Henan Province for Colleges and Universities under Grant No. 2020GGJS172.

Availability of data and materials

The data that support the findings of this study are available from the corresponding author upon reasonable request.

Declarations

Ethics approval and consent to participate

Not applicable.

Consent for publication

Not applicable.

Competing interests

The authors declare that they have no conflicts of interest.

Author details

[1]School of Electronic and Information, Jiangsu University of Science and Technology, Zhenjiang 212003, China. [2]School of Intelligent Engineering, Zhengzhou University of Aeronautics, Zhengzhou 450046, China.

Received: 5 May 2021 Accepted: 3 August 2021

Published online: 18 August 2021

References

1. R. Schmidt, Multiple emitter location and signal parameter estimation. IEEE Trans. Antennas Propag. **34**(3), 276–280 (1986). https://doi.org/10.1109/TAP.1986.1143830
2. D. Ciuonzo, G. Romano, R. Solimene, Performance analysis of time-reversal MUSIC. IEEE Trans. Signal Process. **63**(10), 2650–2662 (2015). https://doi.org/10.1109/TSP.2015.2417507
3. D. Ciuonzo, On time-reversal imaging by statistical testing. IEEE Signal Process. Lett. **24**(7), 1024–1028 (2017). https://doi.org/10.1109/LSP.2017.2704612

4. R. Roy, T. Kailath, ESPRIT-estimation of signal parameters via rotational in variance techniques. IEEE Trans. Acoust. Speech Signal Process. **37**(7), 984–995 (1986). https://doi.org/10.1117/12.55606
5. P. Ma, J. Li, F. Xu, X. Zhang, Hole-free coprime array for DOA estimation: augmented uniform co-array. IEEE Signal Process. Lett. **28**, 36–40 (2021). https://doi.org/10.1109/LSP.2020.3044019
6. P. Pal, P.P. Vaidyanathan, Nested arrays: a novel approach to array processing with enhanced degrees of freedom. IEEE Trans. Signal Process. **58**(8), 4167–4181 (2010). https://doi.org/10.1109/TSP.2010.2049264
7. X. Li, J. Chen, W. Tan, W. Yang, Gridless DOA estimation method for monostatic MIMO array base on covariance matrix reconstruction. Syst. Eng. Electron. **42**(5), 969–977 (2019)
8. S. Qin, Y.D. Zhang, M.G. Amin, Improved two-dimensional DOA estimation using parallel coprime arrays. Signal Process. **172**(Jul.), 107428.1-107428.9 (2020). https://doi.org/10.1016/j.sigpro.2019.107428
9. C. Liu, P.P. Vaidyanathan, Super nested arrays: linear sparse arrays with reduced mutual coupling—part I: fundamentals. IEEE Trans. Signal Process. **64**(15), 3997–4012 (2016). https://doi.org/10.1109/TSP.2016.2558159
10. C. Liu, P.P. Vaidyanathan, Super nested arrays: linear sparse arrays with reduced mutual coupling—part II: high-order extensions. IEEE Trans. Signal Process. **64**(16), 4203–4217 (2016). https://doi.org/10.1109/TSP.2016.2558159
11. J. Liu, Y. Zhang, Y. Lu, S. Ren, S. Cao, Augmented nested arrays with enhanced DOF and reduced mutual coupling. IEEE Trans. Signal Process. **65**(21), 5549–5563 (2017). https://doi.org/10.1109/tsp.2017.2736493
12. G. Wang, Z. Fei, S. Ren, 2D DOA estimation exploiting vertical synthetic planar arrays. IEEE Access **9**, 3497–3507 (2021). https://doi.org/10.1109/ACCESS.2020.3047686
13. Z. Zhang, Y. Guo, Y. Huang, P. Zhang, A 2-D DOA estimation method with reduced complexity in unfolded coprime L-shaped array. IEEE Syst. J. **15**(1), 407–410 (2021). https://doi.org/10.1109/JSYST.2019.2948089
14. J. Li, D. Jiang, X. Zhang, DOA estimation based on combined unitary ESPRIT for coprime MIMO radar. IEEE Commun. Lett. **21**(1), 96–99 (2017). https://doi.org/10.1109/LCOMM.2016.2618789
15. Z. Meng, W. Zhou, Robust adaptive beamforming for coprime array with steering vector estimation and covariance matrix reconstruction. IET Commun. **14**, 2749–2758 (2020). https://doi.org/10.1049/iet-com.2019.1314
16. G. Li, T. Li, M. Xu et al., Sparse massive MIMO-OFDM channel estimation based on compressed sensing over frequency offset environment. EURASIP J. Adv. Signal Process. **2019**, 31 (2019). https://doi.org/10.1186/s13634-019-0627-3
17. Y. Zhou, X. Chen, Y. Li et al., A fast STAP method using persymmetry covariance matrix estimation for clutter suppression in airborne MIMO radar. EURASIP J. Adv. Signal Process. **2019**, 13 (2019). https://doi.org/10.1186/s13634-019-0610-z
18. J. Li, P. Stoica, MIMO radar with colocated antennas. IEEE Signal Process. Mag. **24**(5), 106–114 (2007). https://doi.org/10.1109/MSP.2007.904812
19. F. Wen, Z. Zhang, X. Zhang, CRBs for direction-of-departure and direction-of-arrival estimation in collocated MIMO radar in the presence of unknown spatially coloured noise. IET Radar Sonar Navig. **13**(4), 530–537 (2019). https://doi.org/10.1049/iet-rsn.2018.5386
20. F. Wen, Computationally efficient DOA estimation algorithm for MIMO radar with imperfect waveforms. IEEE Commun. Lett. **23**(6), 1037–1040 (2019). https://doi.org/10.1049/iet-rsn.2018.5386
21. J. Li, L. He, Y. He, X. Zhang, Joint direction of arrival estimation and array calibration for coprime MIMO radar. Digit. Signal Process. **94**, 67–74 (2019). https://doi.org/10.1016/j.dsp.2019.07.002
22. W. Zhou, Q. Wang, J. Wang, DOA estimation for monostatic MIMO radar based on unfolded coprime array. J. Nanjing Univ. Posts Telecommun. Nat. Sci. Ed. **39**(6), 1–8 (2019). https://doi.org/10.1049/el.2016.3818
23. R. Bautista, J.R. Buck, Detecting Gaussian signals using coprime sensor arrays in spatially correlated Gaussian noise. IEEE Trans. Signal Process. **67**(5), 1296–1306 (2019). https://doi.org/10.1109/TSP.2018.2887399
24. W. So, A fast algorithm for 2-D direction-of-arrival estimation. Signal Process. (2003). https://doi.org/10.1016/S0165-1684(03)00118-X
25. N. Tayem, H.M. Kwon, Azimuth and elevation angle estimation with no failure and no eigen decom position. Signal Process. **86**(1), 8–16 (2006)
26. H. Chen, C. Hou, Q. Wang et al., Improved azimuth/elevation angle estimation algorithm for three-parallel uniform linear arrays. IEEE Antennas Wirel. Propag. Lett. **14**, 329–332 (2015). https://doi.org/10.1109/LAWP.2014.2360419
27. D.L. Donoho, Compressed sensing. IEEE Trans. Inf. Theory **52**(4), 1289–1306 (2006). https://doi.org/10.1109/TIT.2006.871582
28. M. Yuan, Model selection and estimation in regression with grouped variables. J. R. Stat. Soc **68**(1), 49–67 (2006)
29. S. Ji, D. Dunson, L. Carin, Multitask compressive sensing. IEEE Trans. Signal Process. **57**(1), 92–106 (2009). https://doi.org/10.1109/TSP.2008.2005866
30. Q. Wu, Y. D. Zhang, M. G. Amin and B. Himed. Complex multitask Bayesian compressive sensing, in *2014 IEEEInternational Conference on Acoustics, Speech and Signal Processing (ICASSP)*, Florence, Italy (2014), pp. 3375–3379. https://doi.org/10.1109/ICASSP.2014.6854226
31. G. C. Cawley and N. L. C. Talbot. Sparse Bayesian learning and the relevance multi-layer perceptron network, in *Proceedings. 2005 IEEE International Joint Conference on Neural Networks, 2005*. Montreal, QC, Canada, vol. 2 (2005), pp. 1320–1324. https://doi.org/10.1109/IJCNN.2005.1556045.
32. S. Ji, Y. Xue, L. Carin, Bayesian compressive sensing. IEEE Trans. Signal Process. **56**(6), 2346–2356 (2008). https://doi.org/10.1109/TSP.2007.914345
33. D.J.C. MacKay, Bayesian interpolation. Neural Comput. **4**(3), 415–447 (1992). https://doi.org/10.1162/neco.1992.4.3.415
34. J. Li, X. Zhang, C. Han, Improved two-dimensional DOA estimation algorithm for two-parallel uniform linear arrays using propagator method. Signal Process. **92**(12), 3032–3038 (2012). https://doi.org/10.1016/j.sigpro.2012.06.010
35. Z. Yi, X. Xu, Y.A. Sheikh et al., A rank-reduction based 2-D DOA estimation algorithm for three parallel uniform linear arrays. Signal Process. **120**(MAR.), 305–310 (2016). https://doi.org/10.1016/j.sigpro.2015.09.019
36. J. Li, D. Jiang, X. Zhang, Sparse representation based two-dimensional direction of arrival estimation using co-prime array. Multidimension. Syst. Signal Process. **29**, 35–47 (2018). https://doi.org/10.1007/s11045-016-0453-9

Publisher's Note